

Electronic Supplementary Information

Influence of dimension and crystallization on visible-light hydrogen production of Au@TiO₂ core-shell photocatalysts based on localized surface plasmon resonance

Bing Liu, Yan Jiang, Yin Wang, Shuxia Shang, Yuanman Ni, Nan Zhang, Minhua Cao* and Chang wen Hu*

Key Laboratory of Cluster Science, Ministry of Education of China, Beijing Key Laboratory of Photoelectronic/Electrophotonic Conversion Materials Department of Chemistry, School of Chemistry and Chemical Engineering, Beijing Institute of Technology, Beijing 100081, P. R. China. E-mail: caomh@bit.edu.cn; cwhu@bit.edu.cn

**To whom correspondence should be addressed.
Email: caomh@bit.edu.cn; cwhu@bit.edu.cn*

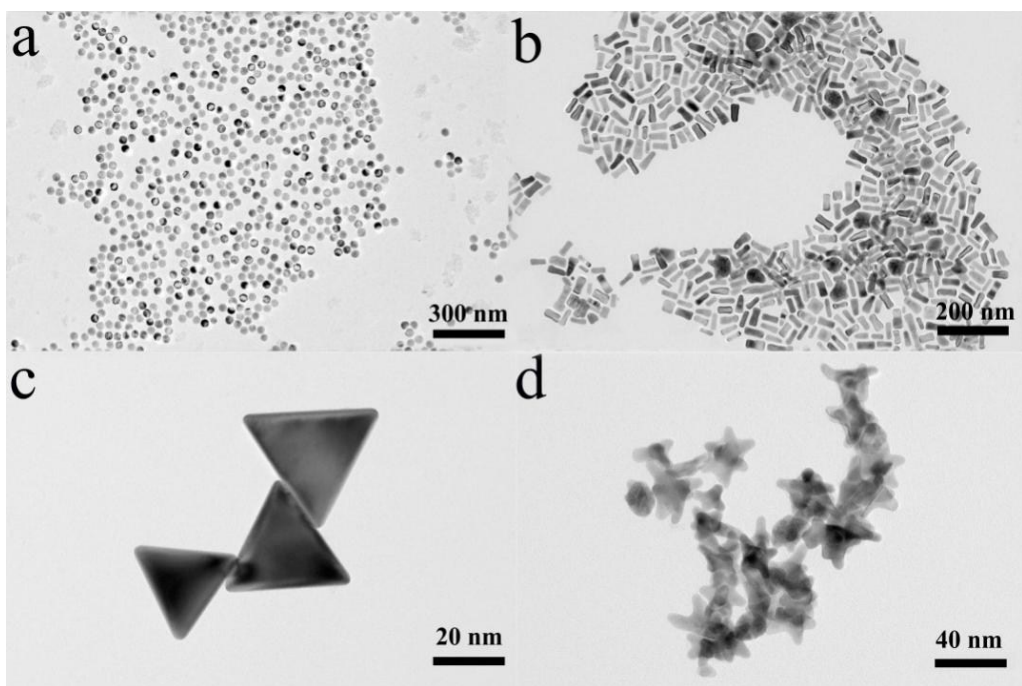


Fig. S1 TEM images of as-prepared Au NPs (a), Au nanorods (b), Au nanoprisms (c), and Au nanostars (d).

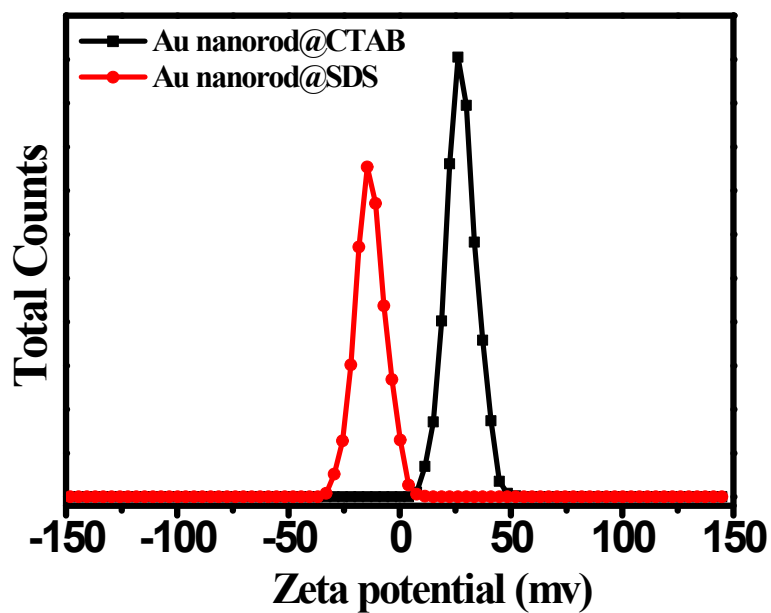


Fig. S2 The Zeta potential of Au nanorods before and after SDS exchange.

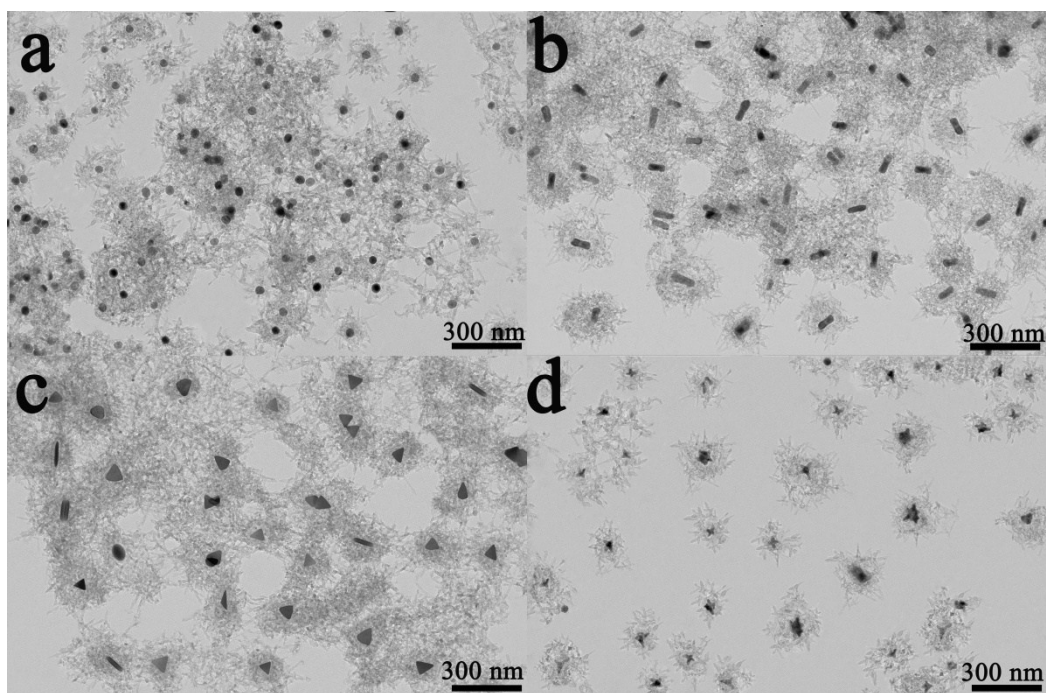


Fig. S3 TEM images of crystallized Au NP@c-TiO₂ (a), Au nanorod@c-TiO₂ (b), Au nanoprism@c-TiO₂ (c), and Au nanostar@c-TiO₂ (d).

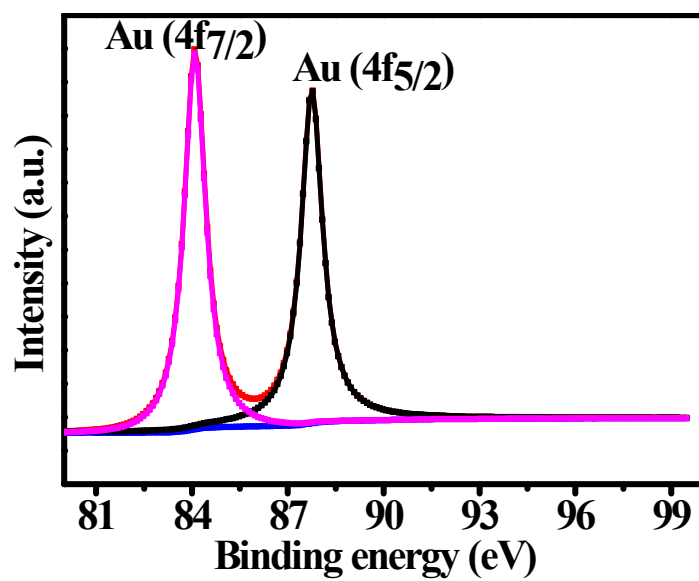


Fig. S4 XPS spectrum of bare Au NPs.

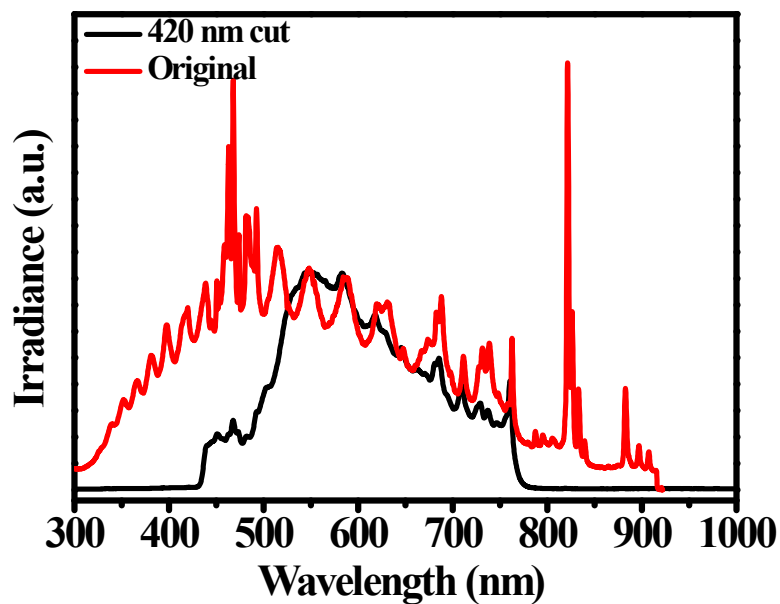


Fig. S5 Emission spectrum of the Xe lamp and its equipped with a UV-cutoff filter that transmits light in the range of $\lambda > 420$ nm.

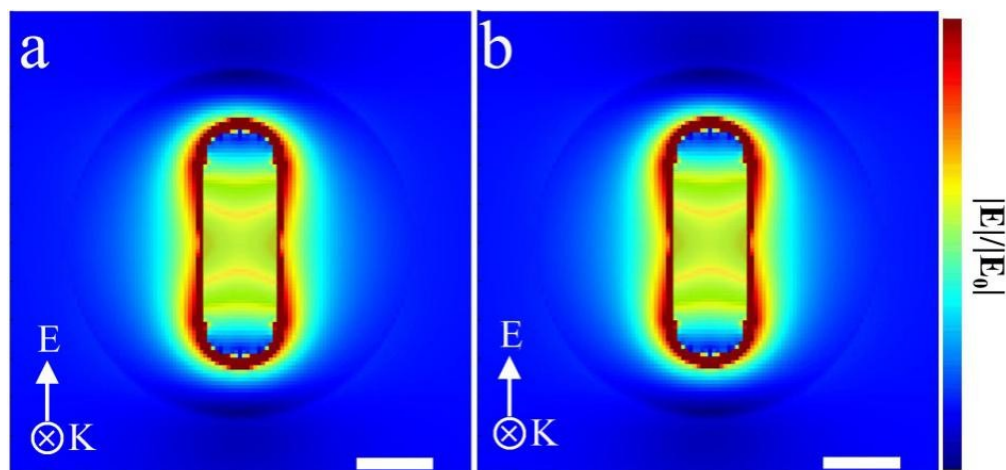


Fig. S6 Plasmonic near-field maps of Au nanorod@c-TiO₂ nanostructures simulated using methanol (a) and water (b) as the surrounding medium. The maps show the electric nearfield intensity enhancements $|\mathbf{E}|/|\mathbf{E}_0|$ at the LSPR wavelength with incident polarization as marked. The results are very similar due to the comparable refractive indices of methanol and water (around 1.328 and 1.33, respectively).

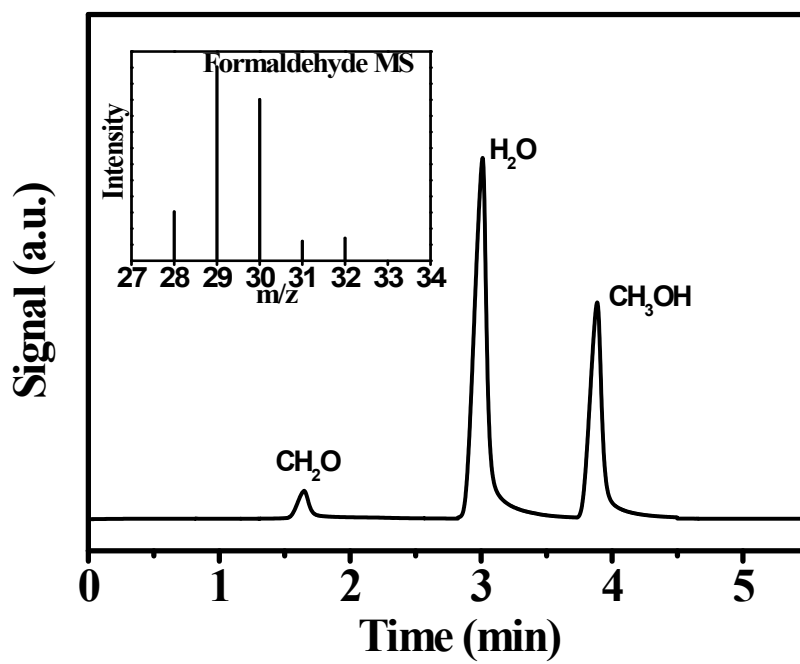


Fig. S7 Gas chromatography-mass spectrometry (GC-MS) of the solution after the photocatalytic reaction. The inset is the mass spectrum of formaldehyde.